

XP-002064986

SAW PLANAR NETWORK

S.C.-C. Tseng, and G. W. Lynch
IBM T. J. Watson Research Center
Yorktown Heights, N. Y. 10598

P.D.

1974

D.

282-285 =

4

An SAW transducer placed between two multi-strip reflectors is operated as a two terminal tank circuit. The device shows resonance and anti-resonance at frequencies where the input voltage is either in phase or out of phase with the back e.m.f. Such a two terminal device can be designed to behave as a single tank circuit, possessing a pole and a zero, or as a series of tank circuits, possessing equally spaced pole-zero pairs. Besides being a suitable replacement for crystal resonators in crystal controlled oscillators, the present device has the capability of operating at fundamental mode in excess of 100 MHz. The SAW tank circuit can be also used to synthesize filter networks. We have made two types of SAW tank circuits in which the zero of one tank circuit coincides with the pole of the other. They are further used as building blocks to construct filters in the configuration of ladder network and lattice networks. Each stage of the network would require at least 4 crystal resonators, if conventional crystal devices were to be used. Experimental results of SAW ladder network and lattice network on LiNbO_3 substrates will be presented and the uniqueness of SAW complete planar networks will be discussed.

Introduction

In this paper, we present our experimental studies of surface acoustic wave planar resonators and related filter networks which are implemented simply by deposition of conductive patterns on a surface of LiNbO_3 substrates.

The planar resonator studied here consists of a surface wave transducer placed between two multi-strip reflectors. Assuming the transducer is equidistance (L') from the reflectors, the surface waves propagating back and forth between the transducer and the reflectors will resonate at cavity modes of

$$f_m = \frac{mv}{2L'} \quad (1)$$

where v is the velocity of the surface waves, m , an integer, and f_m is the m th mode of the cavity resonant frequency. The frequency separation between two adjacent modes is clearly

$$\Delta f_m = \frac{v}{2L'} \quad (2)$$

Multi-mode Resonators

Since the surface acoustic wave is generated and sensed by the transducer, and the transducer itself has a finite bandwidth, not all cavity modes can be excited. Assuming the transducer consists of N pairs of interdigital electrodes, then the frequency bandwidth between the first nulls of the transducer response is

$$\Delta f_x = \frac{2f_0}{N} = \frac{2v}{N\lambda_0} \quad (3)$$

where f_0 is the center frequency and λ_0 is its corresponding wavelength of the transducer. Therefore, the number of modes which can be excited by this device will be

$$n = \Delta f_x / \Delta f_m = 2 \frac{2L'}{N\lambda_0} = \frac{2L}{d} \quad (4)$$

where $L = 2L'$ is the separation between the two reflectors and d is the length of the transducer. Because of the limited page space, we show the experimental verification of Eq. (3) only in the symposium presentation. A multimode resonator such as this can be used for a voltage controlled oscillator which generates discrete frequencies.

Single Mode Resonator

In Eq. (4), as the number of electrode pairs N in the transducer is increased, the number of modes n which can be excited decreases. In order to obtain

a single mode resonator, the following conditions have to be considered.

(A) The number of modes excited should be $n \leq 2$ in Eq. (4), which requires $L = d$. This condition, however, is not physically realizable, because the reflectors have finite dimensions in the direction of wave propagation. Nevertheless, n can be set nearly equal to 3.

(B) With $n = 3$, if one of the cavity modes f_m coincides with the center frequency of the transducer, the f_{m-1} and f_{m+1} modes will be nearly at the first nulls of the transducer response. This requires that $f_m = mv/(2L')$ be equal to the center frequency $f_0 = v/\lambda_0$. Fig. 1-a illustrates the result of such a resonator. In this experimental device, which is made for a feasibility study and not necessarily meant to be optimum, the transducer consists of two 30 pair electrodes connected electrically in series, but acoustically equivalent to a single 60 pair transducer. Such a design enables one to reduce the static capacitance to one-quarter of that of the 60 pair transducer. The finger length of the device is 20 μ , and both the finger width and spacing are 1 mil. Each reflector is a 120 strip structure with half a mil strip width and a half mil space. $L' = 108 \mu$, $d = 60 \mu$ and $n = 3.6$ in this device. The oscillogram of Fig. 1-a shows the current i vs. frequency for a constant input voltage. It is converted into the driving point impedance in amplitude and phase as in Fig. 2. The resonator clearly shows a resonance and an anti-resonance. At the resonance frequency f_r , the phase is zero and the impedance is nearly minimum (a zero in complex S plane). At anti-resonance frequency f_a , the phase is again zero and the impedance is nearly maximum (a pole). The driving point impedance is inductive in the region between f_r and f_a and is capacitive outside this region. This characteristic is very much the same as that of a bulk crystal resonator.

The circuit inertia of a resonator, if defined by

$$Q_0 = \frac{(f_a + f_r)}{2(f_a - f_r)} \quad (5)$$

is $Q_0 = 224$ for the illustrated device. Two such devices connected in series yield $Q_0 = 306$ as in Fig. 3. Note that two devices in series can be reduced into one single planar pattern, and is no more complicated than a single device. At the time this paper is being prepared, observation of anti-

resonance is reported by Lakin et al in a single interdigital transducer without reflectors. The transducer consists of 100 pairs of 5 wavelength electrodes. Their device with a parallel loading capacitance showed a $Q_0 = 78$ according to the data given by Lakin et al, but the inertia defined by

$$Q_a = \frac{f_a}{2} \left| \frac{d\phi}{df} \right|_f \quad (6)$$

is as high as 1900 at $f = f_a$, where $\frac{d\phi}{df}|_f$ is the slope of the phase angle curve evaluated at $f = f_a$.

According to this definition, our single device has a $Q_r = Q_0 = 701$, and $Q = Q_0 = 880$ for two devices connected in series, where Q_r is defined by replacing subscript a by r in Eq. (6). These values are measured directly on the device and no parallel loading capacitance is added. The existence of a shunt loading capacitance lowers the anti-resonance frequency f_r to closer to the resonance frequency f_a and, as a result, the slope of the phase curve increases at f_r . Thus, Q_r can be increased considerably with the definition of Eq. (6). On the other hand, the parallel loading capacitance also increases the direct feedthrough current to such an extent that the series resonance may be completely buried, and Q_0 and Q_r will remain very small. In contrast to such a transducer-only resonator, the existence of the reflectors shown here seem to yield considerably higher Q_0 and Q_r . By optimization of the device and designing it for higher frequency above 100 MHz operation, it should not be difficult to bring the Q_0 and Q_r from 800 at 33.6 MHz to above 2000.

Complementary Resonator

The reason for utilizing reflectors is not just to improve the Q_0 and Q_r as described above. One of the purposes of our study is to utilize the reflectors to control the positions of the resonant (zeros) and the anti-resonant (poles) frequencies. In a lattice filter network, to be discussed later, two types of resonators are required. The poles of one resonator (say device B) must be designed to coincide with the zeros of another (say device A). In principle, this can be achieved by several means. One may consider changing the transducer periodicity in B device slightly from that of A, so that the anti-resonant frequency (f_{rB}) of the B device is shifted to coincide with the resonance frequency (f_a) of the A device. In reality this is very difficult, if not impossible, because the periodicity of the device must differ only by an order of Λ/Λ_0 . Even for resonators having a Q_0 of 100, the fabrication of such a resolution will be impractical. One may also consider the possibility of fabricating the same devices along different crystal orientations on the same surface, so as to utilize two different wave velocities. Again, the fabrication becomes difficult.

In the structure of the present devices, the control of pole-zero relation can be easily achieved as follows. Let the A device be designed to have a resonance frequency f_a which has a cavity length of L'_A , and the B device to have the cavity length of $L'_B = (L'_A - X)$. The resonant frequency of the B device will then be

$$f_{rB} = \frac{L'_A}{L'_A - X} f_{rA}$$

It is desirable that this frequency is equal to the anti-resonance frequency of the A device, f_{aA} . By

equating $f_{rB} = f_{aA}$, we have

$$X = L'_A \left[1 - \frac{f_{rA}}{f_{aA}} \right] \quad (7)$$

Assuming the separation $f_{aA} - f_{rA}$ is approximately equal to one-half the separation of the M^{th} and the $(M+1)^{\text{th}}$ cavity mode of the A device, i.e.,

$$f_{aA} - f_{rA} \approx \frac{1}{2} \frac{v}{2L'_A} = \frac{1}{2} \frac{f_{rA} \Lambda_0}{2L'_A} \quad (8)$$

Eq. (7) is reduced to $X \approx \frac{\Lambda_0}{4}$ for $4L'_A \gg \Lambda_0$.

This conclusion can be also arrived at by simple physical reasoning. The reduction of the cavity length by one-quarter a wavelength will result in one-half wavelength change in the round trip distance by the surface waves in the cavity. Thus the position of peaks and nodes of the standing waves in the cavity will interchange positions. This is experimentally demonstrated in Fig. 1-b. Clearly the positions of the poles and zeros in the B device are complementary to those of the A device. Another uniqueness of such a design is that the static capacitance of the two devices remain exactly equal. This fact is important in lattice network (bridge circuit) applications, when static capacitances of the two arms have to be balanced.

Planar Networks

Besides being a suitable replacement for crystal resonators in crystal controlled oscillators, especially in the higher frequencies, the planar resonators (or SAW tank circuits) can be also used to synthesize filter networks. Once the two aforementioned types of devices are available, ladder networks and lattice networks can be constructed. The simplest examples are a symmetrical T for a section of ladder network and a simple bridge for a section of lattice network. There are many possible variations in the combined use of pure capacitors and tank circuits with complementary pole-zero relation. The complexity of the network depends on the bandwidth and percentage separation ranges required of the networks. The implementation of these networks with crystal resonators have been discussed by Mason⁷. The primary purpose of this study is to show the feasibility of these implementations with SAW circuits and how they can be accomplished with one conductive pattern on a surface of a substrate. If no inductance is allowed, networks realizable with SAW resonators are bandpass filters. Right column of Fig. 4 illustrates the SAW patterns used to realize the networks shown in the left column of the figure. In the T network or the lattice network, both A and B devices shown in Fig. 4 can be either SAW resonators or pure capacitors. Usually, B has the complementary pole-zero configuration with respect to A. In the SAW pattern, we only show the case where the B device is a pure capacitance, to illustrate another unique feature of the SAW implementation. A pure capacitance can be implemented with an interdigital electrode oriented along the X axis of the y-cut z-propagating substrate. Along the X axis the electrode does not generate surface waves, because of the weak piezoelectric coupling. Even if it does, the frequency will be outside the range of our interest. This is very convenient, especially if the value of the capacitance has to be equal to the capacitance of the other arm. Exact capacitance can be obtained by simply rotating the same transducer in the resonator by 90° on the surface of the substrate. For illustration, Fig. 5 is an experimental result of a symmetrical T section. The series arm Z_a is the A

Tseng

device described above and the shunt arm Z_B is a pure capacitance of 40 pf. The pass band of the filter is known to be in the region

$$0 > \frac{Z_A}{Z_B} \geq -1 \quad (9)$$

Since Z_B is always negative (capacitive reactance) and Z_A is positive between f and f_a , the lower cut-off occurs at f . The attenuation peak occurs at anti-resonance f_a , consequently, the upper cutoff occurs at somewhere between f and f_a , at which the inductive reactance of Z_A equals capacitive reactance of Z_B . The upper cutoff can be adjusted by the value of the shunt capacitor.

Another illustration (Fig. 6) is an experimental result of a lattice network in which the series arm Z_A is the A device, and the lattice arm Z_B is the complementary B device mentioned above. The pass band of the filter is known to occur in the region.

$$0 > \frac{Z_A}{Z_B} \geq -\infty \quad (10)$$

The filter property can also be described as follows: The pass band occurs in the region where poles of Z_A coincide with zeros of Z_B or vice versa, and the stop band is the region where poles or zeros of Z_A coincide with poles and zeros, respectively, of Z_B . A critical frequency in Z_A , but not in Z_B , or vice versa, defines a cutoff frequency. The attenuation peaks occur when the impedances of the four arms are balanced as a Wheatston bridge. These characteristics are all shown in the experimental results. Similarly, many more variations of filter networks can be realized. The complexity depends on the bandwidth and percentage separation range required of the filter.

Concluding Remarks

We have shown the feasibility of constructing resonators and related networks with SAW devices. We feel that the following remarks represent the uniqueness of the SAW planar devices.

- 1) Complex RLC network function can be realized with simple electrode film patterns deposited on a surface of a piezoelectric substrate.
- 2) The resonant frequencies are not determined by physical size of the crystal (such as the thickness of a crystal resonator) but by the periodicity of the transducer. Therefore, it is possible to fabricate a high frequency device in excess of 100 MHz.
- 3) In bulk crystal resonators, the ratio of static capacitance to the motional capacitance is fixed and is determined by the crystal property only. The ratio is typically 140 for quartz crystal. This ratio determines the passband width in a filter, which is typically only 0.4%. In planar SAW resonators, C_0 can be adjusted independent of C by series connections of interdigital electrodes in a cavity.
- 4) In the SAW resonators, the resonant frequency is determined by periodicity. For a fixed periodicity, the width and the space ratio can be adjusted, so that the relative ratio of the motional inductance and capacitance can be adjusted to some extent.
- 5) The relative pole zero positions can be adjusted

by cavity length with respect to the transducers.

- 6) The transducer fingers can be weighted to control the multi-mode resonator also.

It seems as if the SAW device has more flexibility in adjusting the tank circuit parameter than crystal resonators.

References

- [1] F. G. Marshall, C. O. Newton, and E. G. S. Paige "Surface Acoustic Wave Multistrip Components and Their Applications," IEEE Trans. on Sonics & Ultrasonics, vol. SU-20, pp 134-143, April, 1973.
- [2] K. M. Lakin, T. Joseph, and D. Penunuri "A Surface Acoustic Wave Planar Resonator Employing an Interdigital Electrode Transducer," Appl. Phys. Lett., vol. 25, pp 363-365, Oct. 1974.
- [3] W. P. Mason, "Electro-mechanical Transducers and Wave Filters", 2nd Edition, D. Van Nostrand Co. New York.

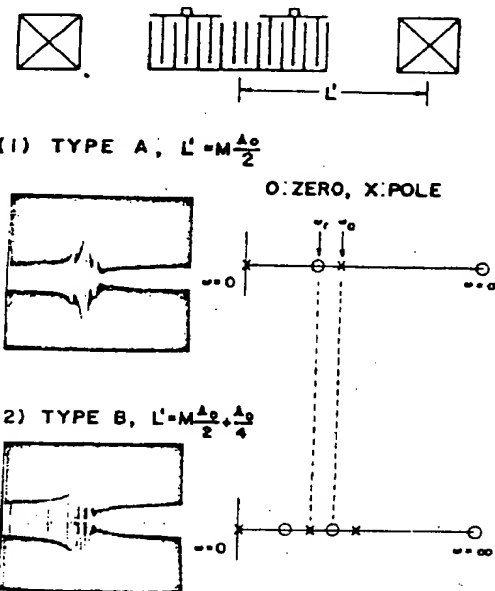


Fig. 1 Two types of resonators whose internal pole-zero positions, are complementary to each other. The cavity lengths of the two differ by $\lambda_0/4$

Tseng

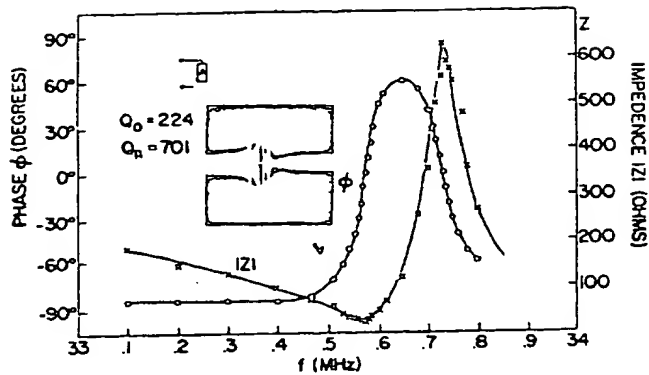


Fig. 2 Driving point impedance of a single resonator A.

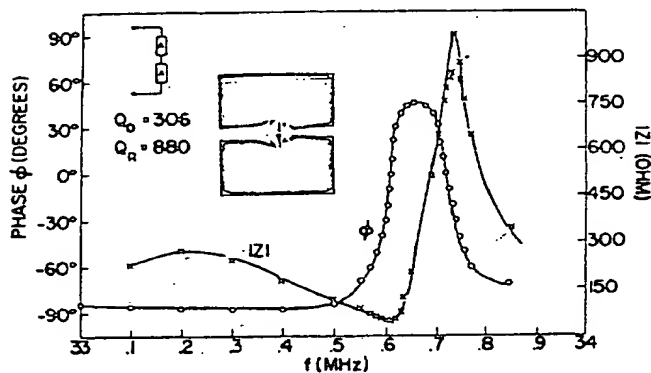
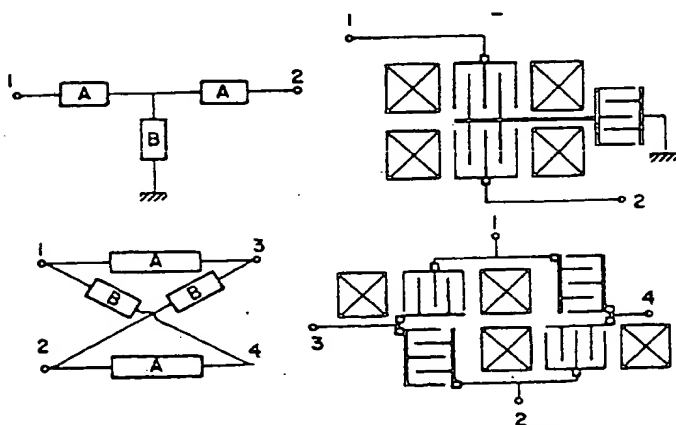
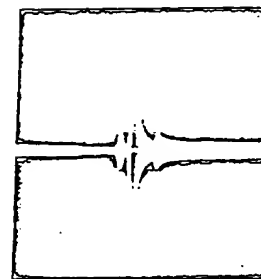


Fig. 3 Driving point impedance of two A devices in series



SAW IMPLEMENTATION OF NETWORKS

Fig. 4



Insert of Fig. 5

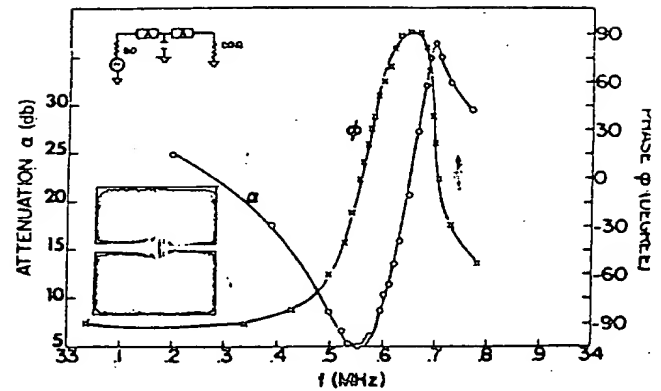


Fig. 5 Transfer characteristics of a T network.

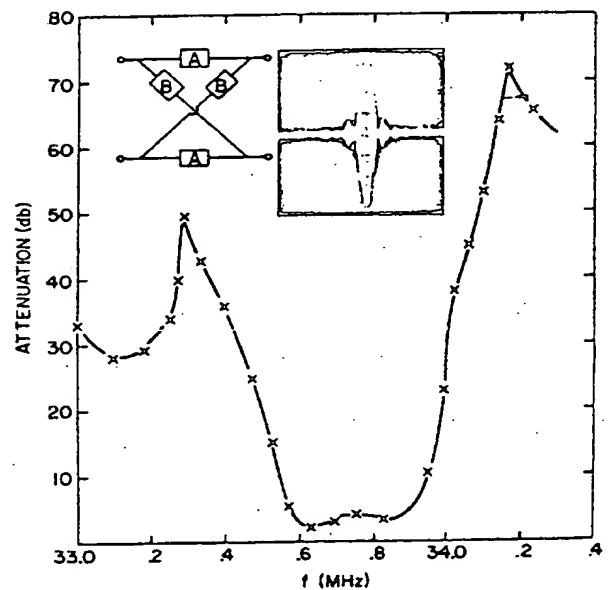


Fig. 6 Transfer characteristics of a lattice network